Targeting cystalysin, a virulence factor of Treponema denticola-supported periodontitis

(Article begins on next page)

28 February 2025

Targeting cystalysin, a virulence factor of *Treponema denticola*-supported periodontitis

Francesca Spyrakis[a]±∞, Barbara Cellini[b]∞, Stefano Bruno[c]∞, Paolo Benedetti[d], Emanuele Carosati[e], Gabriele Cruciani[e], Fabrizio Micheli[f], Antonio Felici[f], Glen E. Kellogg[h], Pietro Cozzini[a][i], Carla Borri Voltattorni[b], and Andrea Mozzarelli[c][i]*

[a]Department of Food Sciences, University of Parma, Parma, Italy, [b]Department of Life Sciences and Reproduction, Section of Biological Chemistry, University of Verona, Verona, Italy, [c]Department of Pharmacy, University of Parma, Parma, Italy, [d]Molecular Discovery Limited, London HA5 5NE, U.K., [e]Department of Chemistry, University of Perugia, Perugia, Italy, [f]Aptuit S.r.l, Verona, Italy, [h]Department of Medicinal Chemistry, Institute of Structural Biology and Drug Discovery, Virginia Commonwealth University, Richmond, Virginia, USA, [g]Italian National Institute of Biostructures and Biosystems.

± Present address: Department of Life Sciences, University of Modena and Reggio Emilia, Modena, Italy

∞These authors equally contributed to the work.

* Corresponding authors: Andrea Mozzarelli, Department of Pharmacy, University of Parma, Parco Area delle Scienze 23/A, 43124 Parma, Italy. Phone 0039-0521905138; Fax 0039-0521905151, Email: andrea.mozzarelli@unipr.it

Barbara Cellini, Department of Life Sciences and Reproduction, Section of Biological Chemistry, University of Verona, Verona, Italy. Phone 0039-045-8027293; Fax 0039-045-8027170; E-mail: barbara.cellini@univr.it

Keywords: pyridoxal 5'-phosphate, cystalysin, microspectrophotometry, in silico screening, enzyme inhibitor

Abbreviations

pyridoxal 5'-phosphate, PLP; aminoethoxyvinylglycine, AVG; virtual screening, VS; ligand-based virtual screening, LBVS; structure-based virtual screening, SBVS; Molecular Interaction Fields, MIFs; Cation-Adjust Mueller Hinton Broth, CAMHB.

Abstract

Cystalysin from *Treponema denticola* is a pyridoxal 5'-phosphate-dependent lyase that catalyzes the formation of pyruvate, ammonia and sulfide from cysteine. It is a virulence factor in adult periodontitis because its reaction contributes to hemolysis, which sustains the pathogen. Therefore, it was proposed as a potential antimicrobial target. To identify specific inhibitors with structure-based *in silico* methods, we first validated the crystal structure of cystalysin as a reliable starting point for the design of ligands. By using single crystal absorption microspectrophotometry, we found that the enzyme in the crystalline state, with respect to that in solution, exhibits: i) the same absorption spectra for the catalytic intermediates; ii) a close pK_a value for the residue controlling the ketoenamine ionization; and iii) comparable reactivity with glycine, L-serine, L-methionine, and the aspecific irreversible inhibitor aminoethoxyvinylglycine. Next, we screened *in silico* a library of 9,357 compounds using the three-dimensional structure of cystalysin as template. Seventeen compounds were selected and experimentally evaluated by enzyme assays and spectroscopic methods. Two compounds were found to competitively inhibit recombinant *T. denticola* cystalisin, with K_i values of 25 and 37 μM. One of them exhibited a MIC value of 64 μg/mL on *Moraxella catarrhalis* ATCC23246, proving its ability to cross bacterial membranes.

Introduction

Treponema denticola is a gram-negative, obligate anaerobic, motile and highly proteolytic bacterium, associated with the incidence and severity of human periodontal disease. *T. denticola* is related to the syphilis-causing obligate human pathogen, Treponema pallidum subsp. Pallidum and is highly specialized to survive in the oral environment[Jobin, 2008 #83]**.** *T. denticola* expresses cystalysin [E.C.4.4.1.1], an enzyme that, by catalyzing the α,β-elimination of L-cysteine to give pyruvate, ammonia and sulfide, enables the bacterium to produce sulfide at millimolar concentrations in the periodontal disease pocket[Chu, 1997 #16212]. Sulfide, in turn, is responsible for hemolytic and hemoxidative activities[Chu, 1999 #16210; Kurzban, 1999 #16211] and for the damage to the gingival and periodontal tissues[Zhang, 2010 #16213]. Moreover, sulfide creates an ecological niche that selectively benefits *T. denticola*. Therefore, cystalysin can be considered as a virulence factor and represents a potential target for the development of new drugs for the treatment of periodontitis[Kurzban, 1999 #16211; Amadasi, 2007 #8816].

Cystalysin is a homodimeric pyridoxal 5'-phosphate (PLP)-dependent lyase and belongs to the Fold Type I group of PLP-dependent enzymes[Grishin, 1995 #16200]. Each monomer consists of a large domain (residues 48-288), which includes Lys238, to which the cofactor is covalently bound, and a small domain (residues 1-47 and 289-394), formed by the two terminal regions of the polypeptide chain (Fig. 1)[Krupka, 2000 #16201].

Recent extensive biochemical studies have highlighted the high catalytic versatility of cystalysin[Bertoldi, 2002 #16206; Bertoldi, 2003 #16204; Bertoldi, 2003 #16205; Cellini, 2003 #16203; Cellini, 2005 #16209; Cellini, 2004 #16202; Cellini, 2006 #16208]. Besides its physiologically relevant eliminase activity, cystalysin catalyzes the racemization of both enantiomers of alanine, with a turnover number of seconds, and the half-transamination of L- and D-alanine, with a turnover number of minutes. In addition, the enzyme is able to perform the β-desulfination of L-cysteine sulfinic acid and the β-decarboxylation of both L-aspartate and oxalacetate.

The catalytic mechanism proposed for the α,β-elimination performed by cystalysin involves the initial formation of the external aldimine, followed by C_α-deprotonation to give the carbanionic quinonoid intermediate. Then, sulfide elimination generates the PLP-derivative of aminoacrylate that, after protonation and reverse transaldimination steps, yields iminopropionate and the enzyme-bound PLP. Iminopropionate is released from the active site and hydrolyzed to pyruvate and ammonia[Krupka, 2000 #16201].

Cystalysin exhibits absorption bands at 418 and 320 nm, attributed to the ketoenamine form of the internal aldimine and to a substituted aldamine, respectively[Bertoldi, 2003 #16205]. The characterization of the spectral changes occurring during the interaction of cystalysin and its mutant Y64A with substrates and substrate analogs allowed for the identification of several reaction intermediates of the α,β-elimination, including an external aldimine absorbing at 330 nm and the α-aminoacrylate species[Cellini, 2005 #16209]. Several substrate analogs were found to bind to the cystalysin active site in an unproductive mode, thus preventing the elimination reaction at different steps along the catalytic pathway[Bertoldi, 2002 #16206]. Glycine blocks the reaction at the level of the external aldimine, as indicated by the shift of the visible absorbance band of the enzyme from 418 to 429 nm, whereas L-methionine and L-homoserine form equilibrium mixtures of external aldimine and quinonoid species absorbing at 429 and 508 nm, respectively.

Although cystalysin represents an attractive pharmacological target, no specific exogenous inhibitor has been identified so far. In order to identify novel inhibitors with potential therapeutic activity, we first compared the spectroscopic and functional properties of the enzyme in solution and in the crystalline state by absorption microspectrophotometry[Mozzarelli, 1998 #16423; Mozzarelli, 1996 #16216; Pearson, 2004 #16215; Pearson, 2011 #16214; Ronda, 2011 #16217; Bruno, 2001 #16222; Phillips, 2002 #16223; Storici, 2004 #16220; Moniot, 2008 #16219; Kaiser, 2003 #16221], validating the currently available crystal structures of cystalysin[Krupka, 2000 #16201]. Afterwards, we predicted *in silico* the affinity for the enzyme of thousands of exogenous small molecules and we selected the most promising ones to evaluate their inhibitory activity with *in vitro*

assays[Spyrakis, 2013 #9162]. Finally, for the best inhibitors, we determined the MIC values on a panel of bacteria to evaluate both activity and cell permeability.

Results and Discussion

Reactivity of cystalysin in the crystalline state. *In silico* screening methods for the identification of potential enzyme ligands are based on either the matching between active site and compound pharmacophore or the compound complementarity with the active site, assessed by docking and scoring. For both approaches, the quality of the structural data is critical for the success rate of analysis[Cozzini, 2002 #16272]. Therefore, before carrying out the *in silico* screening, we have validated the available three-dimensional structure of cystalysin by characterizing the enzyme reactivity in crystals grown under the same conditions as those used for crystal growth and characterization[Krupka, 2000 #16201]. The single crystal absorption spectrum of cystalysin exhibits a well-defined band centered at 417 nm, as in solution[Cellini, 2003 #16203] (Fig. 2), attributed to the ketoenamine tautomer of the internal aldimine. The native spectrum was found to be pH-dependent (Fig. 2), with the intensity of the band at 417 nm decreasing at increasing pH values, and with the concomitant increase of the intensity at 318 nm. As previously found in solution, no isosbestic point is present at 370 nm, indicating that more than two interconverting species are present[Cellini, 2003 #16203]. The pH dependence is controlled by a single ionizable residue with a pK_a of 8.5 (Fig. 2, inset), as in solution[Cellini, 2003 #16203]. It was suggested that the ionizable group is either a residue involved in the formation of the aldimine or another group, the ionization of which influences the equilibrium between the species absorbing at 417 and 320 nm[Cellini, 2003 #16203]. These findings indicate that the active site geometry, including the position of the group controlling the pH-dependent species interconversion, is not perturbed by crystallization.

In solution, cystalysin reacts with substrate analogues, leading to the accumulation of distinct catalytic intermediates, depending on the chemical nature of their leaving group[Cellini, 2003 #16203]. The reaction of glycine with cystalysin's internal aldimine leads to the accumulation of the external aldimine that absorbs at 429 nm,[Cellini, 2003 #16203] because glycine does not possess a β-eliminating moiety. The exposure of cystalysin crystals to increasing concentration of

glycine caused a shift of the absorption band from 417 nm to 429 nm (Fig. 3A), indicating the formation of the external aldimine. The isotherm of binding yields a dissociation constant of 6.3 ± 0.3 mM (Fig. 3A, inset), a value comparable to that found in solution, 1.92 ± 0.09 mM[Cellini, 2003 #16203].

Upon incubation of cystalysin crystals in a solution containing an increasing concentration of L-serine, the absorption band at 417 nm shifts to 429 nm (Fig. 3B), as observed for glycine, indicating the formation of the external aldimine. However, in the presence of L-serine, the band is broader on the red side, suggesting the formation of a small amount of a quinonoid species. These findings are in full agreement with the reactivity observed in solution,[Cellini, 2003 #16203] where a mixture of the catalytic intermediates external aldimine and quinonoid species was observed. Unlike glycine, L-serine is a substrate, undergoing deamination to pyruvate and ammonia. Indeed, it is a very poor substrate with a k_{cat}/K_M ratio that is about 1400 fold lower than L-djenkolic acid, the best cystalysin substrate[Cellini, 2003 #16203]. The apparent dissociation constant for L-serine to cystalysin in the crystal is 16 ± 2 mM (Fig. 3B, inset), a value comparable with that estimated in solution, 7 ± 1 mM[Cellini, 2003 #16203].

Upon incubation of cystalysin crystals in a solution containing increasing concentrations of L-methionine, the absorption band at 417 nm decreases without a shift of the peak wavelength, accompanied by the concomitant formation of a small band at 510 nm, diagnostic of the presence of a quinonoid species (Fig. 3C). These findings are fully consistent with those observed in solution[Cellini, 2003 #16203]. The dissociation constant for L-methionine in the crystal is 33 ± 5 mM (Fig. 3C, inset), close to the value determined in solution, 44 ± 4 mM[Cellini, 2003 #16203].

The reaction of cystalysin crystals with AVG, a PLP-dependent non-specific enzyme inhibitor, was investigated by monitoring spectra as a function of time (data not shown). The absorption band at 417 nm was completely abolished in the presence of saturating concentrations of AVG, with the concomitant appearance of a band at 340 nm, attributed to a ketimine species[Krupka, 2000 #16201]. This species is very stable, as the resuspension of cystalysin crystals in an AVG-free

solution did not modify the absorption spectrum. This finding confirms the high stability of the AVG-cystalysin complex and its inability to undergo a complete transamination reaction, as observed in the X-ray crystallographic study of the cystalysin-AVG complex[Krupka, 2000 #16201].

Active site anatomy of cystalysin. The active sites of holo-cystalysin (PDB code 1c7n) and the AVG-cystalysin complex (1c7o) are shown in Fig. 4A and 4B, respectively. The estimated volumes of the PLP-AVG complex and of the ligand binding pocket are 326 Å^3 and 693 Å^3, respectively. The inspection of the binding site of the cystalysin–AVG complex (Fig. 4B) reveals the presence of several unoccupied crevices, located near the PLP pyridine nitrogen and the PLP phosphate group, which could be occupied by properly designed ligands. In order to better evaluate the potential interactions of a ligand within the binding pocket, GRID MIFs were calculated using a hydrophobic, an H-bond acceptor and an H-bond donor probe, corresponding, respectively, to the green, blue and red contours (Fig. 4C). The two regions, highlighted by the red and blue contours located in front of Arg369 and Asp355, represent two hot spots and a potential target of cystalysin ligands. Another interesting area is above the PLP phosphate group, where a H-bond donor or acceptor group could be placed. Also the side-chains of Tyr123, Tyr124 and Tyr485 might accept interacting groups. On the other hand, the blue contour lying close to Asp660 is possibly too far from the pocket core and from the previously described hot spots to be occupied by incoming ligands. Finally, a large hydrophobic area (green contour) is lined by Leu21, Val99, Phe103, Pro125, Tyr458, Met128, Met665 and Phe667, with the Tyr458 phenyl ring representing a possible site for π-π interactions. Overall, the cystalysin active site contains polar and non-polar residues and unoccupied volumes; all of which make the search of specific ligands worthwhile.

Structure-based Virtual Screening (SBVS) on cystalysin. The structure-based screening on the filtered Specs database was performed with FLAP[Baroni, 2007 #16250; Baroni, 2007 #16250] using the holo-cystalysin structure (1c7n)[Krupka, 2000 #16201]. The protein binding pocket and

the related Molecular Interaction Fields (MIFs) represent the template. A first SBVS was performed by directly screening the 9,357 compounds into the protein binding pocket defined by the FLAPsite algorithm, implemented into FLAP. Then, the database was enriched by adding tautomers and protomers built with the Moka algorithm, [Milletti, 2007 #16257; Milletti, 2010 #16258; Cruciani, 2009 #16256] to obtain a total of 14,018 compounds. Ligands were ranked according to the FLAP distance to the template,[Cross, 2010 #16310] a global score representing the overall similarity based on a combination of the degree of the overlap between the single MIFs computed on the ligand and the template, i.e. the protein binding site. The top 2% ligands were visually inspected and the most interesting molecules, according to the chemical and steric similarity with the template, were docked into the cystalysin binding pocket with GOLD[Jones, 1995 #16425] and then rescored with HINT[Kellogg, 2001 #16261] for a consensus scoring evaluation, an approach that we have reported previously [25,53,54] to be successful in identifying small molecule and peptide candidates with high affinity.

On the basis of: i) the generated conformations, ii) the superimposition with the pocket's MIFs iii) the interactions with the surrounding residues, iv) the HINT score value and v) the chemical diversity, seventeen compounds were selected for testing (Table 1).

Enzyme inhibition assays. The seventeen compounds identified by virtual screening (Table 1) were purchased and tested as inhibitors of recombinant cystalysin at their maximal solubility concentration. The inhibition degree was strong (100%) for compounds **1** and **2**, medium (21-60%) for compounds **3-6**, weak (8-20%) for compounds **7-9** and negligible for compounds **10**-**17**.

The dependence of the inhibitory activity as a function of compounds **1** and **2** concentrations (Fig. 5A) allowed determination of IC_{50} values 33 ± 3 μM and 17 ± 3 μM, respectively. Their inhibition profile revealed a competitive inhibitor behavior, with K_i values of 25 ± 3 μM (Fig. 5B) and 37 ± 6 μM (Fig. 5C), respectively.

Furthermore, the spectral changes associated to the binding of compounds **1** and **2** were investigated. Upon addition of a saturating concentration of compound **1** to purified recombinant cystalysin, we observed: (i) a modest increase of the absorbance band at 418 nm, and the disappearance of the shoulder at 320 nm (data not shown), probably due to the formation of the enzyme-ligand complex; and (ii) a 60% quenching of the intrinsic tryptophan fluorescence intensity (Fig 6A). These findings suggest that the interaction of compound **1** with the active site of cystalysin gives rise to a conformational change involving Trp residues. Cystalysin contains eight Trp residues per monomer: five are in the large domain and three in the small domain. The inspection of the crystal structure reveals that none of them is in the enzyme active site, thus, it is not possible to assign the intrinsic fluorescence quenching caused by the binding of compound **1** to the movement of a specific Trp residue. Rather, an indirect effect of the change of the active site microenvironment on the orientation of one or more Trp residues can be suggested. In this regard, it should be mentioned that all the cystalysin ligands previously tested induce, even at a different extent, a quenching of intrinsic tryptophan fluorescence. This observation was interpreted as due to small changes in the relative orientation of PLP and aromatic residue(s) occurring upon ligand binding (Bertoldi et al. biochemistry 2002). Accordingly, in the crystal structure of L-aminoethoxyvinylglycine-liganded cystalysin the pyridine ring of PLP rotated slightly with respect to the position of the unliganded enzyme, without observing any gross structural changes or domain movements (Kupta et al). The dependence of the intrinsic fluorescence quenching on the concentration of compound **1** (Fig. 6A, inset), fitted to equation 1, yielded a K_D value of 74 ± 13 μM, in agreement with the K_i value determined by inhibition of the catalytic activity. At saturating concentrations, compound **2** caused a significant decrease in tryptophan fluorescence (data not shown) as well as in the absorbance band at 418 nm, with the formation of a band at 320 nm (Fig. 6B). The dependence of the absorbance at 320 nm as a function of compound **2** concentration (Fig. 6B, inset), fitted to equation 1, yielded a K_D value of 12 ± 2 μM, in agreement with the K_i value determined by inhibition of the catalytic activity. Similarly to the decrease in fluorescence

observed for compound **1**, compound **2** caused a significant quenching of tryptophan fluorescence (data not shown), suggesting a change in the active site microenvironment that in turn alters the position of Trp residues (see above).

Docked models of cystalysin ligands vs inhibitory activity. The seventeen compounds contain at least a hydrogen acceptor moiety, i.e., a carboxylic group or an isoster, or a nitro group, able to interact with the Arg369 side chain (Table 1, Table 1S). Moreover, they contain an apolar moiety capable of occupying the hydrophobic cleft lined by Leu21, Val38, Pro125, Met128, Tyr485, Met665 and Phe667. Most of them also contain a second hydrogen bond acceptor group presumed to be oriented towards Tyr123 and Tyr458 side chains, or towards the PLP phosphate (Table 1S). Some of them may also be able to form an additional hydrogen bond with the carboxylic moiety of Asp355. These features are consistent with the pharmacophore properties of the binding site previously described (Fig. 4c).

All of the seventeen compounds exhibit molecular weights between 176 and 288 Da, most of them possess an aromatic moiety (except compounds **6, 7** and **17**) and many have two carboxylic groups. Their docking models are reported in Table 1S (supporting Information), where polar and hydrophobic interactions are highlighted; here we discuss only compounds **1** and **2**, and use the superposition of ligand's atoms with the corresponding GRID MIFs to aid the structure-based analysis of the ligand-protein interactions occurring into the protein active site.

Docking predictions show that compound **1** (Fig 7A) interacts with both Arg369 and Asp355 through the sulfonic group and properly fills the hydrophobic patch defined by Val99, Pro125, Met128, Tyr458 and Phe667. In addition, the sulfonic group lies both in the H-bond acceptor regions (red contours) in front of Arg369, and in the H-bond donor contour (blue contour) in front of Asp355, while the dihydro indolic group occupies the hydrophobic-favorable area (green contour). Similarly, docking predictions show that compound **2** interacts with both Arg369 and

Asp355 through the sulfonylhydrazide moiety, forming, as compound **1**, two parallel hydrogen bonds (Fig. 7B). Moreover, the availability of a free amine might allow for the formation of a Schiff base with PLP.

Compounds **1** and **2** well fulfill the requirement of a H-bond acceptor group placed in front of Arg369 (red contour) and a H-bond donor group in front of Asp355 (blue contour). The two compounds have a thiosulfate and a sulfonohydrazide moiety, respectively, suggesting that the presence of a sulfone interacting with Arg369 well stabilizes the formation of a cystalysin-ligand complex. Also, an additional group able to contact Asp355 seems to represent a basic condition for the protein-ligand interaction, which is a property also shared by compounds **13**, **16** and **17**. Nevertheless, the unfavorable placement of the other groups, i.e., polar moieties into hydrophobic contours and hydrophobic moieties into polar contours, likely counteracts the enzyme inhibition.

Compounds possessing only carboxylic groups, i.e., **3**, **4**, **6**, **7**, **8**, **9**, **11**, **12**, **14** and **15**, gave lower or no inhibition. Tetrazole rings, isosteres of the carboxylic groups (compounds **5** and **10**), also do not give good inhibitory effects. A number of docking models report carboxylic groups close to Tyr123 and Tyr458 (Table 1S). Nevertheless, these contacts do not appear to provide a significant contribution to cystalysin inhibition, as suggested by the small volume of the corresponding H-bond acceptor contour (small red contour in Fig. 4C). The presence of a hydrophobic moiety filling the hydrophobic patch formed by Val99, Pro125, Met128, Tyr458 and Phe667 (main green contour in Fig. 4C) appears to be essential for tight binding. This peculiarity is, more or less, fulfilled by all the seventeen selected molecules, with the exception of compounds **3**, **7** and **13**. Unfavorable interactions given by the placement of polar groups in hydrophobic contours (compounds **5**, **13** and **17**) or hydrophobic groups into polar contours (compounds **4**, **7**, **8**, **11**, **12**, **14** and **17**) also disadvantage any complex formation (Table 1S).

Overall, in order to provide a significant inhibition of the enzyme, compounds need to contact Arg369, and possibly Asp355, and to properly fill the pocket's hydrophobic patch. Our fast computational procedure has been quite successful in identifying cystalysin inhibitors with

dissociation constants of the best hits in the micromolar range from a relatively small library, and with large/wide chemical diversity. This finding supports the strength of VS approaches, which allow for the identification of scaffolds with significantly different features to be exploited in the following optimization steps. The same procedure has allowed to identify inhibitors of the PLP-dependent enzyme O-acetylserine sulfhydrylase with dissociation constants in the micromolar range,[Spyrakis, 2013 #16224] and similar approaches have been successfully used to identify inhibitors of human DOPA decarboxylase[Daidone, 2012 #16270] and serine hydroxymethyltransferase[Daidone, 2011 #16269]. In accord with the orientations assumed by the ligands into the model provided by GOLD, and, most of all, with the extension of the MIFs calculated by FLAP, modifications could be introduced in order to optimize compounds towards the corresponding target.

Antibiotic activity of compounds 1 and 2. The evaluation of the antimicrobial activity of compounds **1** and **2** was carried out for a panel of 14 bacteria strains (Table 2). The panel of strains was selected with the aim of evaluating the potential of the chemical class to inhibit growth of community and acquired infection pathogens. Since cystalysin is a virulence factor of *T. denticola*, which is produced during infection, we assume that no in vitro activity would have been found. Whereas compound **1** did not show any antibiotic activity up to 128 μg/mL, a MIC of 64 μg/mL was observed for compound **2** against *Morax catarrhalis* ATCC23246, that is known to be highly sensitive towards any class of compounds exerting antibacterial activity. This result indicates that compound **2** is able to cross bacterial membranes and to display an antibiotic activity, although with a low potency. The estimated LE value for compounds 1 and 2 is respectively 0.39 and 0.43, thus perfectly falling in the range of ligand efficiency for known protein inhibitors [Reynolds, 2008 #88]. This indicates compound 2 as a more promising inhibitor than compound 1 and calls for an optimization campaign in order to increase its activity. Nevertheless, we are also aware that LE and many other "optimization" functions, such as SILE, LELP, lipE, are unable of "catching" the

complexity of ligand binding concerted events, depending not only on the number of heavy atoms (or on molecular weight) of the ligand and of the binding energy [Schultz, 2013 #89].

A structural comparison of cystalysin from *T. denticola* with other PLP enzymes indicates a similarity in overall folding with a PLP-dependent C-S lyase from *Corynebacterium diphtheriae*, a pathogenic bacterium that causes diphtheria [Astegno, 2013 #87]. This observation opens the possibility of testing the potency of compound **2** also on this bacterium.

Conclusions

This work is the initial step toward the development of cystalysin inhibitor, potentially useful as antibiotic agents. Cystalysin is very relevant for the survival of *T. denticola* as it provides a strategy to lysate red blood cell and, thus, to obtain the iron contained in hemoglobin that is essential for the bacterial survival and proliferation. Moreover, only *T. denticola* is able to survive at the millimolar concentration of sulfide produced by cystalysin, thus creating a suitable ecological niche with respect to other bacteria. Therefore, the targeting of cystalysin is a worthwhile effort because it may lead to a decreased fitness of the bacteria within the infection site, and may make common antibiotics more effective. This approach has been pursued in the case of the *O*-acetylserine sulfhydrylase, the enzyme that synthesizes cysteine in *Salmonella thyphimurium* [Turnbull, 2010 #84], and is at the basis of the strategies that are targeting sulfur assimilation enzymes [Bhave, 2007 #85][Spyrakis, 2013 #29][Amori, 2012 #86][Spyrakis, 2013 #25].

Experimental section

Chemicals. Bis-Tris propane, Mg-acetate, glycine, L-serine, L-methionine and β-chloro-L-alanine were purchased from Sigma-Aldrich. PEG 4000 was purchased from Hampton Research. Aminoethoxyvinylglycine (AVG) was a kind gift of Dr. Roberto Contestabile, University of Rome, 'La Sapienza'. All reagents were of the best commercial quality available. Compounds predicted to bind to cystalysin were purchased from Specs (Delft, The Netherlands, www.specs.net). The purity of the compounds (90% or higher) was confirmed by NMR and/or LC-MS data provided by the vendor.

Expression and purification of T. denticola cystalysin. *T. denticola* cystalysin was expressed and purified as previously described.[Bertoldi, 2002 #16206] The enzyme concentration was determined using an ε_M of 1.277 x 10^5 $M^{-1}cm^{-1}$ at 281 nm[Bertoldi, 2002 #16206; Bertoldi, 2002 #16206]. The PLP content was determined by releasing the coenzyme in 0.1 M NaOH and using the ε_M = 6600 $M^{-1}cm^{-1}$ at 388 nm.

Cystalysin crystal growth. Cystalysin crystals were grown according to Krupka et al.[Krupka, 2000 #16201] from PEG 4000 solutions. The crystals exhibit a rhombic shape belonging to the monoclinic space group $P2_1$[Krupka, 2000 #16201].

Microspectrophotometric measurements. Absorption microspectrophotometric measurements on cystalysin single crystals were carried out as previously described[Mozzarelli, 1996 #16216; Pearson, 2004 #16215; Ronda, 2011 #16218]. Before measurements, cystalysin crystals were suspended in a solution containing 25% PEG 4000 (w/V), 0.2 M Mg-acetate, 20 mM Bis-Tris propane buffered at the desired pH. Polarized absorption spectra were recorded with linearly polarized light parallel to either the *a* or *b* crystal axes. Because spectra collected along the two directions were indistinguishable, unpolarized light was used thereafter.

The effect of pH on absorption spectra of cystalysin crystals was evaluated by re-suspending crystals in a solution containing 25% PEG 4000 (w/V), 0.2 M Mg-acetate, 20 mM Bis-Tris propane buffered at different pHs ranging from 6.0 to 9.6. At pH 9.6 the titration was not complete due to crystal damage. The pK_a was determined by fitting the dependence of peak absorbance intensity as a function of pH values to the equation for a sigmoidal curve.

Binding of glycine, L-serine and L-methionine was monitored by recording absorption spectra of a cystalysin crystal suspended in a soaking solution containing 25% PEG 4000 (w/V), 0.2 M Mg-acetate, 20 mM Bis-Tris propane buffered at pH 7.4 and increasing ligand concentrations. Bis-Tris propane buffer was selected because the phosphate buffer used for the experiments in solution was incompatible with the high concentrations of Mg-acetate, the co-precipitating agent present in the crystallization medium. The dissociation constant was estimated by fitting the dependence of peak absorption as a function of ligand concentration to a binding isotherm.

The reaction of cystalysin crystals with AVG was monitored by resuspending crystals in a solution containing 0.1 mM AVG, 25% PEG 4000 (w/V), 0.2 M Mg-acetate, 20 mM Bis-Tris propane buffered at pH 6.5, and recording absorption spectra as a function of time.

Molecular Modeling.

Virtual screening (VS). The Specs database (www.specs.net) was chosen as the library for performing VS. This database is part of the ZINC archive [Irwin, 2005 #16246] (www.zinc.docking.org) and, according to previous recent experiences [Carosati, 2006 #16311; Brincat, 2011 #16249; Carosati, 2012 #16248; Spyrakis, 2013 #9162], it provides affordable molecules in terms of purity and availability. The database contains molecules with significant chemical and geometric diversity. A set of about 300,000 compounds was downloaded and filtered according to their calculated LogP values. In fact, preliminary VS analyses, performed without any LogP filter, led to the selection of compounds difficult to manage in the experimental assays. Therefore, in order to assure sufficient solubility, only molecules with calculated LogP ≤ 0.8 were

retained, leaving 9,357 compounds in the pool. The library was then incremented by adding tautomers and protomers with Moka[Milletti, 2007 #16257; Milletti, 2010 #16258; Cruciani, 2009 #16256] up to 14,018 compounds.

The VS was performed with FLAP (Fingerprints for Ligands and Proteins) software,[Baroni, 2007 #16250; Cross, 2010 #16251] developed and licensed by Molecular Discovery Ltd. (www.moldiscovery.com). The FLAP approach[Cross, 2010 #16310], based on the Molecular Interaction Fields (MIFs) calculated by GRID[Goodford, 1985 #16244; Carosati, 2004 #16245], has been successfully applied in several VS analyses[Muratore, 2012 #16253; Muratore, 2012 #16252; Sirci, 2012 #16254; Spyrakis, 2013 #9162; Spyrakis, 2013 #16224]. This procedure allows selecting the most interesting candidates with chemical and structural complementarity with the receptor binding site and/or its known ligands (see Supplementary Materials).

Given the unavailability of cystalysin structures complexed with non-covalent ligands, i.e. the only available enzyme-ligand complex is formed by cystalysin and the AVG covalent inhibitor (PDB code 1c7o) [Krupka, 2000 #16201], a receptor-based pharmacophore model was built with cystalysin holo-form (PDB code 1c7n) [Krupka, 2000 #16201] and used as template for structure – based virtual screening (SBVS) analyses.

Compounds were ranked according to the distance from the template.[Cross, 2010 #16251] The most interesting molecules were docked with GOLD[Goodford, 1985 #16244] and then rescored with HINT[Kellogg, 2001 #16261; Kellogg, 2001 #16261; Spyrakis, 2004 #9817; Amadasi, 2006 #9811; Spyrakis, 2007 #16237; Spyrakis, 2013 #9162; Ahmed, 2011 #9782; Ahmed, 2013 #16225; Kellogg, 2001 #16261; Salsi, 2010 #9168; Cozzini, 2002 #16272; Cozzini, 2002 #16272]. HINT was used as a rescoring function based on our previous studies indicating a higher reliability of HINT scoring with respect to other scoring functions, and its successful use in the search of ligands for other targets [Spyrakis, 2007 #74][Spyrakis, 2007 #47][Spyrakis, 2013 #29][Spyrakis, 2004 #77][Spyrakis, 2013 #25][Amadasi, 2008 #41].

Activity assay of cystalysin in the absence and presence of ligands. Cystalysin lyase activity was determined by measuring the production of pyruvate upon reaction with β-chloro-L-alanine in a spectrophotometric assay coupled with L-lactate dehydrogenase, as previously reported.[Cellini, 2003 #16203] The reaction was carried out at 25 °C in a 20 mM potassium phosphate buffer containing 50 nM enzyme, at pH 7.4. To determine the concentration required to inhibit 50% of enzyme activity (IC_{50}), assays were carried as a function of compound concentration, at β-chloro-L-alanine concentrations close to its K_M. Activity assays were carried out in duplicate. IC_{50} values were derived by nonlinear regression analysis. The inhibition mode of the more active compounds was determined by measuring the rate of the α,β-elimination reaction in the absence or presence of fixed amounts of each compound. The K_i values were determined from a non-linear cumulative fit of the curves using the software Prism 5.0 (GraphPad software, San Diego, CA, USA). Various amounts of dimethyl sulphoxyde (DMSO) were necessary to solubilize the compounds in 20 mM potassium phosphate buffer, pH 7.4. The final DMSO concentration in the assay mixture was kept lower than 10% (v/v), i.e., under experimental conditions that do not affect the lyase activity.

Spectroscopic measurements. Absorbance measurements were carried out with a Jasco V-550 spectrophotometer using 1 cm path length quartz cuvettes. Fluorescence measurements were performed with a Jasco FP750 spectrofluorometer using 5 nm excitation and emission bandwidths. Spectra of the blanks, i.e. of samples containing all components except cystalysin, were recorded before measurements and subtracted from enzyme-containing spectra.

Determination of the enzyme-ligand dissociation constant (K_D). The K_D of compounds for cystalysin was determined by monitoring as a function of ligand concentration either the decrease in the intensity of the intrinsic fluorescence emission at 330 nm of a solution containing 1 μM enzyme, 20 mM potassium phosphate buffer, pH 7.4, or the increase in the absorbance intensity at 320 nm of a solution containing 5 μM enzyme, 20 mM potassium phosphate buffer, pH 7.4. The maximum

DMSO concentration in the mixture was kept lower than 10% (v/v). The K_D values were obtained by fitting data to the equation for a tight binding isotherm:

$$Y = Y_{MAX} \times \frac{[E]_t + [L]_t + K_D - \sqrt{([E]_t + [L]_t + K_D)^2 - 4[E]_t[L]_t)}}{2[E]_t}$$

(1)

where $[E]_t$ and $[L]_t$ represent the total concentrations of cystalysin dimer and ligand, respectively, Y isthe intrinsic fluorescence emission intensity or the absorbance at 320 nm at the ligand concentration [L], and Y_{max} is the fluorescence or absorbance signal when all enzyme sites are complexed with the ligand.

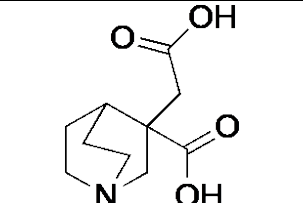### *Determination of MIC values for selected compounds.*
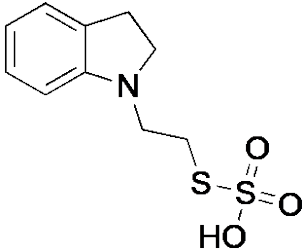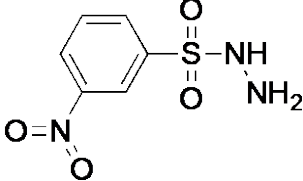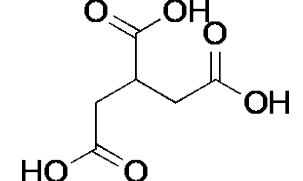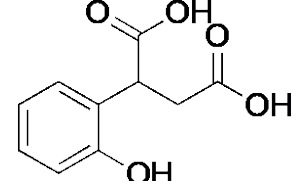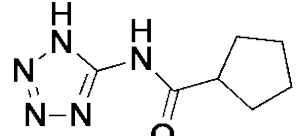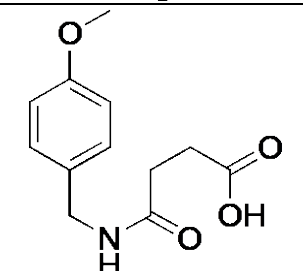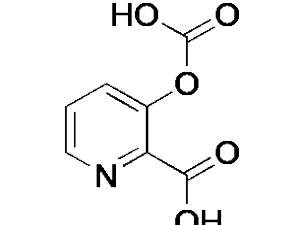
Compounds were dissolved in dimethyl sulfoxide (DMSO) at 5.12 mg/mL, diluted 1:20 in Cation-Adjust Mueller Hinton Broth (CAMHB). Then, 12 two-fold serial dilutions in CAMHB were performed. The concentration range of 0.06-128 µg/mL was tested. The panel of gram positives and gram negatives bacterial strains used is reported in Table 2.

Non-fastidious strains were tested in CAMHB and fastidious strains were tested in CAMHB plus 2.5% of Lysed Horse Blood. *Haemophilus* strain was tested in Haemophilus Test Medium as recommended in M07-A8 Clinical and Laboratory Standard Institute guidelines.

The Broth Microdilution Method according to M07-A8 guidelines was used to determine MIC values. Briefly, 50 µL of the two times test inoculum (range 2 to 8×10^5 CFU/mL) prepared in CAMHB from direct colony suspension of an overnight culture plate of each bacterial strain was dispensed aseptically to the wells of 96-well microtiter plates containing 50 µL of doubling dilution of test compounds. The plates were incubated at 35 ± 2 °C in ambient air and read after 20 to 24 hours. Negative controls (no bacterial cells) and growth control wells were included in the plates. MIC values, expressed as µg/mL, were determined as the lowest concentration required for

complete growth inhibition (no visible growth). Ciprofloxacin was included as internal standard for assay quality control.

Table 1

cpd	Specs code	Structure	HINT score	Ligand (mM)	% Inhibition	Ki (μM)
1	AE-848/07784001		2318	4.63	100	25 ±3
2	AI-942/25034272		3108	1.16	100	37 ± 6
3	AI-942/42301799		1208	4.93	41	
4	AE-842/32538023		1388	4.18	22	
5	AK-968/40947382		1316	1.39	22	
6	AQ-360/42595885		1028	1.13	21	
7	AJ-333/09217010		985	5.25	18	
8	AE-641/00361044		1143	16.9	17	
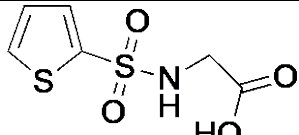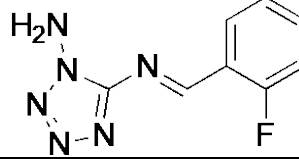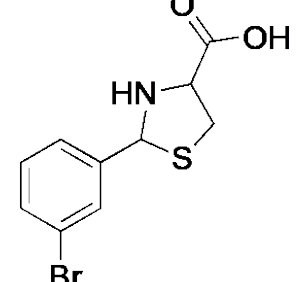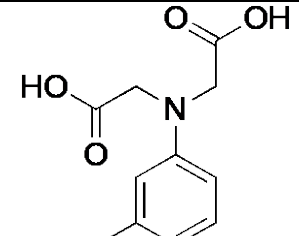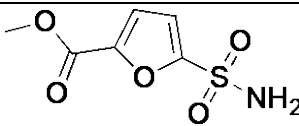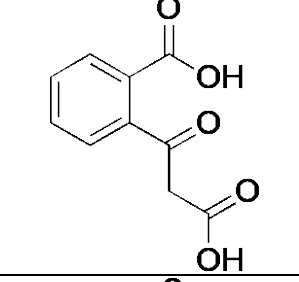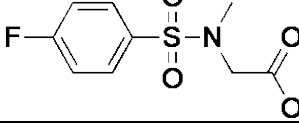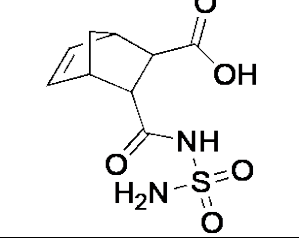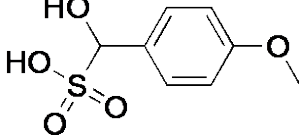
9	AQ-390/42133048		1676	2.43	15	
10	AG-670/31512063		1270	0.86	7	
11	AH-487/13096054		1257	0.18	5	
12	AK-918/10656024		1154	1.43	4	
13	AL-281/40679323		1740	3.27	1	
14	AC-907/34133001		1417	0.15	0	
15	AO-080/41006208		1615	2.16	0	
16	AO-623/14653131		1968	3.70	0	
17	AG-690/33036043		1781	4.85	0	

Table 2. Evaluation of antibacterial activities of compounds 1 and 2.

Organism	Phenotype	Compound 1 (µg/ml)	Compound 2 (µg/ml)
Staph.aureus ATCC29213		>128	>128
Staph.aureus	Met-R; Pen-R	>128	>128
Staph.aureus	MLSc	>128	>128
Strep.pyogenes	MLSc; Pen-S	>128	>128
Strep.pyogenes	M; Pen-s	>128	>128
Strep.pyogenes	Ery-S; Pen-S	>128	>128
S. pneumoniae ATCC 49619		>128	>128
S. pneumoniae	Ery-S; Pen-S	>128	>128
S. pneumoniae	Ery-R; Pen-R	>128	>128
E.coli ATCC25922		>128	>128
Haem.influenzae ATCC49247		>128	>128
K. pneumoniae ATCC43816		>128	>128
Pseudo. aeruginosa ATCC27853		>128	>128
Morax.catarrhalis ATCC23246		>128	64

Acknowledgments

References

Figure legends

Fig. 1. Ribbon-tube representation of the native cystalysin homodimer (PDB code 1c7n). [Krupka, 2000 #16201] The PLP cofactor is displayed in yellow capped sticks.

Fig. 2. pH-dependence of internal aldimine cystalysin crystals. The titration was carried out by resuspending the same crystal in a solution containing 25% (w/v) PEG 4000, 0.2 M Mg acetate, 20 mM Bis-Tris propane, adjusted at the desired pH values, at 20 °C. Representative spectra recorded at pH 6.0 (solid line), 8.0 (dotted line), 8.8 (dash-dot line) and 9.4 (dash-dot-dot line) are shown. The spectral changes are fully reversible. Inset: Absorbance at 318 nm (triangles) and 417 nm (circles) as a function of pH. The curve through data points is the fitting to the equation for a single ionizable residue with a pK_a of 8.5 ± 0.3.

Fig. 3. Titration of the internal aldimine cystalysin crystals with glycine **(a)**, L-serine **(b)** and L-methionine **(c)**. Titrations were carried out by resuspending crystals in a solution containing 25% (w/v) PEG 4000, 0.2 M Mg-acetate, 20 mM Bis-Tris propane and increasing concentrations of amino acids, pH 7.4, at 20 °C. Spectra of the internal aldimine (solid line) and the derivative obtained at saturating concentrations of the amino acids (dashed line) are shown. Insets: dependence of the ratio (R) of the absorbances at 435 and 420 nm (a), at 418 and 429 nm (b) and 509 and 420 nm (c) on the amino acids concentrations. Data points were fitted to binding isotherms, yielding dissociation constants of 6.3 ± 0.3 mM for glycine, 16 ± 2 mM for L-serine and 33 ± 5 mM for L-methionine.

Fig. 4. Cystalysin binding pocket. **A.** Residues lining the binding pocket represented in capped

stick. The PLP is highlighted in yellow, the pocket volume, identified by FLAPsite, is defined by green mesh contours. **B.** AVG complexed with PLP (yellow capped sticks) into cystalysin binding pocket. **C.** The green, red and blue meshed contours represent the favourable binding site regions for placing, respectively, hydrophobic, hydrogen bond acceptor and hydrogen bond donor groups, as calculated by the GRID algorithm.[Carosati, 2004 #16245; Goodford, 1985 #16244] The "hot spot" residues are labelled and represented in capped sticks, with the exception of Tyr223 and Tyr224 for clarity.

Fig. 5. Cystalysin activity in the presence of compounds **1** and **2**. **a)** Cystalysin activity was measured at increasing concentrations of compound **1** (open circle) and compound **2** (closed circles) in an assay solution containing 50 nM cystalysin, 1.2 mM β-chloro-L-alanine, 300 μM NADH, 0.8 μg/μL L-lactic dehydrogenase, 20 mM potassium phosphate, pH 7.4, at 25°C. The IC_{50} values for compound 1 and 2 were 32 ± 3 μM and 17 ± 3 μM, respectively. **b)** Cystalysin activity as a function of β-chloro-L-alanine concentration was determined in the absence (closed circle) and presence of 18.5 (open circle), 46.0 (inverted triangle) and 90.8 mM (triangle) of compound **1**. In the absence of compound 1, the values of K_M and k_{cat} were 2.0 ± 0.2 mM and 71 ± 1 s^{-1}, respectively. The cumulative fitting of the curves provides a value of K_i of 25 ± 3 μM. **c)** Cystalysin activity as a function of β-chloro-L-alanine concentration was determined in the absence (closed circle) and presence of 36.0 (open circle), 43.0 (inverted triangle), and 87.0 mM (triangle) of compound **2**. The cumulative fitting of the curves provides a value of K_i of 37 ± 6 μM.

Fig. 6. Spectral changes of cystalysin in the presence of compounds **1** and **2**. **a)** Fluorescence emission spectra (exc. 280 nm) of a solution containing 1 μM cystalysin, 20 mM potassium phosphate buffer, pH 7.4, at 25 °C, in the absence (solid line) and in the presence (dashed line) of 220 μM compound **1**. Inset. Dependence of the fluorescence intensity at 330 nm as a function of compound **1** concentration. Data points were fitted to a binding isotherm with K_d of 74 ± 13 μM. **b)**

Absorption spectra of a solution containing 10 µM cystalysin, 20 mM potassium phosphate buffer, pH 7.4, at 25 °C, in the absence (solid line) and in the presence (dashed line) of 360 µM compound **2**. Inset. Dependence of the absorbance intensity at 320 nm as a function of compound **2** concentration. Data points were fitted to a binding isotherm with K_d of 12 ± 2 µM.

Fig. 7. Docked model of compounds **1 (a)** and **2 (b)** into the cystalysin binding site. Compounds are represented in capped sticks. Hydrogen bonds are displayed in black dashed lines. MIFs are reported as green (hydrophobic), blue (H-bond donor) and red (H-bond acceptor) contours.